Electroanalytical Study of Active Species to Deposit Ti Alloy from 1-Butyl-3-Methylimidazolium Chloride-Aluminum Chloride Ionic Liquid

ECS Transactions, 98 (10) 231-243 (2020)
10.1149/09810.0231ecst ©The Electrochemical Society

Electroanalytical study of Active Species to Deposit Ti Alloy from 1-Butyl-3-methylimidazolium Chloride-Aluminum Chloride Ionic Liquid

Pravin S. Shinde[a], Yuxiang Peng[a], and Ramana G. Reddy[a]

[a] Department of Metallurgical and Materials Engineering,
The University of Alabama, Tuscaloosa, AL 35487, USA
Corresponding author: rreddy@eng.ua.edu; Tel: 205-348-4246

The electrochemical behavior of titanium-chloroaluminate anion species in Lewis acidic 1-butyl-3-methyl imidazolium chloride (BMIC)-aluminum chloride ($AlCl_3$) ionic liquid (IL) electrolyte with 0.667 $AlCl_3$ mole fraction is investigated at 383K by cyclic voltammetry (CV), chronoamperometry (CA), and chronopotentiometry (CP). The effect of scan rate on peak potential and peak current, constant current density, constant applied potential, and the electrolyte temperature are discussed. The redox reaction of the Ti^{2+}/Ti^0 deposition from titanium hepta-chloroaluminate ($[Ti(Al_2Cl_7)_4]^{2-}$) anions is a reversible process with a 2-electron transfer while that of Al^{3+}/Al^0 deposition from hepta-chloroaluminate ($[Al_2Cl_7]^-$) anions is quasi-reversible with the 3-electron transfer. The cyclic voltammograms indicated that the reduction of $[Al_2Cl_7]^-$ and $[Ti(Al_2Cl_7)_4]^{2-}$ species to corresponding Al and Ti forms is a diffusion-controlled phenomenon. The diffusion coefficients (*D*) of the anion-species in BMIC-$AlCl_3$ IL determined at 383 K using CV and CP methods are 9.74×10^{-10} m^2 s^{-1} and 6.36×10^{-10} m^2 s^{-1}, respectively.

Introduction

Titanium (Ti) is the ninth most abundant element and fourth among common metals in the earth's crust. The Ti and its alloys have been widely employed in aerospace, military, automotive, medical, and several other fields due to their excellent thermomechanical properties such as low density, exceptional strength, high melting point, and good oxidation resistance and structural stability. The Kroll process invented in the 1940s has been the primary method of Ti production (1). Several research efforts have been focused on developing a cost-effective approach to produce low-cost and high-purity titanium (2-12). Electrochemical synthesis from low-temperature ionic liquid (IL) electrolytes is one of the fascinating methods of producing Ti metal or its alloys (13). Unfortunately, the electrochemical mechanism for titanium deposition is more complicated than other metals such as aluminum because of its different oxidation states (II, III, and IV). Therefore, it is often electrodeposited in the form of alloys, such as titanium aluminide (Ti-Al). The ILs are still continuously receiving a lot of scientific interest due to their lack of understanding at the fundamental molecular level, e.g., the ion-ion interactions, leading to different observed properties (14, 15). In general, density, viscosity, electrochemical potential window, and conductivity are important physical properties that determine if an IL is suitable for a given application. Our research group has been

instrumental in studying several physicochemical properties such as the heat capacity (16), thermal stability (17-19), density (20, 21), viscosity (18, 20, 21), vapor pressure (21), thermal conductivity (21, 22), thermodynamic (23-25), and electroanalytical (26-29) properties of several ILs and molten salts, which are necessary to understand the electrochemistry of metals and alloys to tune their electrosynthesis parameters. Electrodeposition of Ti and its alloys from low-temperature ILs, especially in chloroaluminate-based alkyl imidazolium chloride, is very challenging as the electrochemistry of Ti in such IL is very complicated. Such ILs are used to electrodeposit Al using a eutectic mixture of $AlCl_3$ with alkyl imidazolium chlorides (30-34). For instance, in an IL consisting of BMIC and $AlCl_3$, several anion species such as $[AlCl_4]^-$, $[Al_2Cl_7]^-$, and $[Al_2Cl_{10}]^-$ with different concentrations are in equilibrium for a given mole fraction (X_{Al}) of $AlCl_3$. The amount of X_{Al} dictates the acidity or basicity of electrolyte and impacts the electrodeposition conditions. At higher $AlCl_3$ (X_{Al} >0.5), the electrolyte mainly possesses $AlCl_4^-$ and $Al_2Cl_7^-$ species exhibiting Lewis acidic properties primarily due to coordinately unsaturated $Al_2Cl_7^-$ species (35). The electrochemical deposition of Al from such chloroaluminate ILs has been reported to be primarily due to contribution from the diffusion of $Al_2Cl_7^-$ species (34, 36, 37). Acidic IL compositions are active for Al plating and stripping at the anode, according to the reversible redox reaction given below (38, 39).

$$4[Al_2Cl_7]^- + 3e^- \leftrightarrow Al\ (Cathode) + 7[AlCl_4]^- \quad [1]$$

Our group previously performed the electrodeposition of Ti-Al alloys from BMIC-$AlCl_3$-$TiCl_4$ (1:2:0.019 molar ratio) at different applied potentials voltages (1.5-3.0 V) and temperatures (343-398 K) (11). Ti foils were used as cathode and anode, and Ti wire was used as a reference electrode. The possible reactions are given by Eq. (2-5)

$$\text{Cathode reactions: } [Ti(Al_2Cl_7)_4]^{2-} + 2e^- \leftrightarrow Ti\ (Cathode) + 7[AlCl_4]^- \quad [2]$$
$$4[AlCl_4]^- + 3e^- \leftrightarrow Al\ (Cathode) + 7[AlCl_4]^- \quad [3]$$

$$\text{Anode reactions: } Ti\ (Anode) + 4[Al_2Cl_7]^- - 2e^- \leftrightarrow [Ti(Al_2Cl_7)_4]^{2-} \quad [4]$$
$$AlCl_3 + 4[AlCl_4]^- - 3e^- \leftrightarrow 4[Al_2Cl_7]^- + 1.5\ Cl_2 \quad [5]$$

The electrochemical process of reduction of Al-species in the ILs is relatively well studied. However, there are no reports on electrochemical studies of ILs to deposit Ti-Al alloy without the addition of $TiCl_4$ with regard to studying the nucleation and growth mechanisms. In our previous work, the potentiostatic electrodeposition of smooth, compact, and dendrite-free growth of Ti-Al alloy on the copper substrate was demonstrated at −1.3 V vs. Ti for 1 h using BMIC-$AlCl_3$ IL with $AlCl_3$ mole fraction of 0.667 at low temperature (40). However, nucleation and growth mechanisms at constant potential and current densities were not performed.

In this work, the electrodeposition behavior, especially the initial crystallization nucleation and growth mechanism of the Ti-Al alloy electrodeposition on Pt wire electrodes from IL electrolyte consisting of a eutectic mixture melt of BMIC and $AlCl_3$ are investigated using a CV, CA, and CP techniques. Furthermore, the diffusion coefficient (D) values are estimated from using CV and CP methods. The CA experiments are performed to analyze the mechanism of diffusion and nucleation of Ti-Al-species

from BMIC-$AlCl_3$ IL. The diffusion coefficient of $[Ti(Al_2Cl_7)_4]^{2-}$ or $Al_2Cl_7^-$ ions in BMIC-$AlCl_3$ IL with $AlCl_3$ mole fraction of 0.667 are calculated and compared using CP and CV methods at 383 K.

Experimental

Materials

The chemicals such as anhydrous $AlCl_3$ (95%, Alfa-Aesar) and organic chloride salt 1-butyl-3-methylimidazolium chloride (BMIC, 98%, Sigma-Aldrich, HPLC grade) were purchased and used as received. The Pt wire (0.5 mm diameter, 99.99%) was obtained from Sigma Aldrich company. Pure titanium wire (0.25 mm diameter, 99.99%) was obtained from Alfa Aesar®. The ultrahigh pure (UHP) Argon gas (99.999%) was obtained from Airgas.

Preparation of BMIC-$AlCl_3$ Ionic Liquid

The appropriate amount of BMIC organic chloride salt and the $AlCl_3$ were weighed for a given $AlCl_3$ mole fraction. Here, the $AlCl_3$ mole fraction of 0.667 was chosen to maximize the concentration of $Al_2Cl_7^-$ anion species in the BMIC-$AlCl_3$ IL. Both the ingredients were mixed in a Pyrex beaker on a preheated hot-plate. The mixing is performed cautiously and slowly using a glass rod as the spontaneous reaction is vigorous. The mixture of two solid ingredients turns into a clear liquid as the eutectic condition is reached at room temperature. Upon stirring for 30 s, the mixture turns into a clear liquid, although few large chunks of BMIC might float in the solution, which eventually dissolves in about 30 min. The desired amount of clear IL solution is then transferred to the 50 mL electrochemical Pyrex cell placed on a hot plate, and IL was stirred for about 30 min using a magnetic stirrer at 60 RPM for homogeneous mixing at the set temperature. The IL was stored in a dry box until used for further measurements such as density and electrical conductivity. The $AlCl_3$ mole fraction (X_{Al}) of 0.667 in BMIC-$AlCl_3$ IL and at a fixed electrolyte temperature of 383 K was chosen for the electrochemical measurements. The UHP argon gas was purged over the surface of IL to keep it free from oxygen and moisture, and the cell is sealed.

Electrochemical Measurements

The electrochemical measurements were performed from BMIC-$AlCl_3$ IL at 383K using CV, CA, and CP methods using an EG&G PARC model 273A potentiostat/galvanostat instrument controlled by Power Suite software. The electrochemical cell for the measurements consisted of a 40 mL Pyrex® glass beaker fitted with Teflon/Perspex cover, which has provisions for introducing electrodes, thermometer, and inert gas inlet and outlets, as shown schematically in Figure 1.

The experiments were performed from BMIC-$AlCl_3$ IL using a three-electrode cell configuration, where Pt wire served as working electrode (WE), Ti wire as the counter electrode (CE), and Ti or Pt wire as a quasi-reference electrode (RE). The Ti-species

were incorporated from the electrolysis experiment for one hour before starting the electrochemical measurements. The working distance between WE and CE was 0.025 m. The temperature was controlled by a hot plate and was precisely monitored by the inserted thermometer. The Ar gas flow was continuously maintained through the alumina tube during the experiment. All the electrodes were polished with 800-grit SiC abrasive paper, washed with acetone and deionized water, and then dried by air right before the experiment. The height of the electrode immersed in the IL was measured after the experiment.

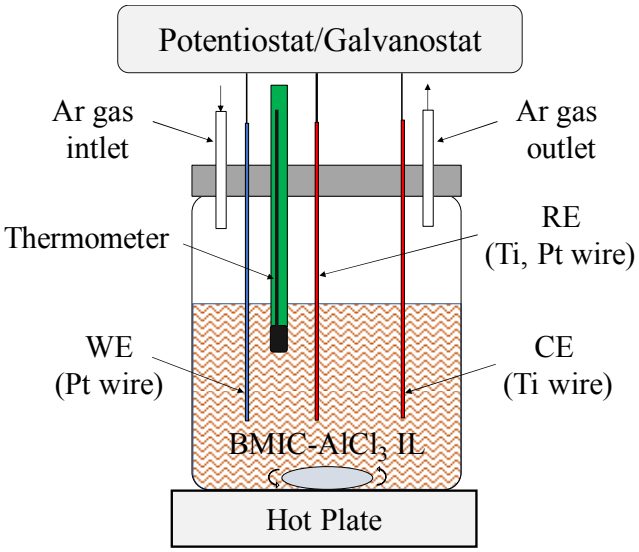

Figure 1. Schematic of the electrochemical cell set-up for CV, CP, and CA experiments in BMIC-$AlCl_3$ IL.

Results and Discussion

Cyclic Voltammetry (CV)

The nucleation and growth studies of metals or alloys are commonly investigated by electroanalytical methods such as CV and CA, which can be served both as the deposition method as well as the diagnostic tools for determining the reaction mechanisms. One can predict the growth models using the experimental measurements, based on certain assumptions involving the nucleation mode (instantaneous, progressive), the dimensional type of growth (2D, 3D), the geometry of growth centers, and the rate-determining step of the entire process. The electrochemical synthesis parameters such as electrolyte temperature, viscosity, and concentration of ionic species play a critical role by controlling the nucleation and growth of electrodeposits in electrodeposition. The diffusion or mass transfer coefficient of ionic species in the IL is one such essential parameters. As mentioned earlier, $Al_2Cl_7^-$ are predominant ionic species in BMIC-$AlCl_3$ IL at an $AlCl_3$ molar fraction of 0.667. Therefore, it is necessary to understand the mass transfer or diffusion of such ions and their complexes to/from the bulk electrolyte to the electrode surface during electrodeposition.

The cyclic voltammograms are obtained from BMIC-$AlCl_3$ IL at Pt electrode with Ti as reference and Ti as a sacrificial anode at 383K. The scan rates are varied from 100 to 300 mV s^{-1}. Figure 2 shows the cyclic voltammograms recorded on polished Pt wire at different scan rates from BMIC-$AlCl_3$ IL. The area of WE immersed inside the electrolyte was 0.118×10^{-4} m^2. The reduction and oxidation peaks are seen in the CV curves. When the CV is swept from 1 V or open circuit potential towards a negative direction, a tiny reduction peak at 0.187 V vs. Ti appears. This peak is due to the two-electron reduction of Ti-hepta-chloroaluminate complex ions from ionic liquid according to reaction [2] to deposit metallic Ti on a copper substrate. As the potential sweeps further toward more negative potentials, the cathodic current becomes steady until −1.0 V vs. Ti and increases rapidly, giving rise to a reduction peak at −1.4 V vs. Ti, which signifies the deposition of Al according to the reaction [3].

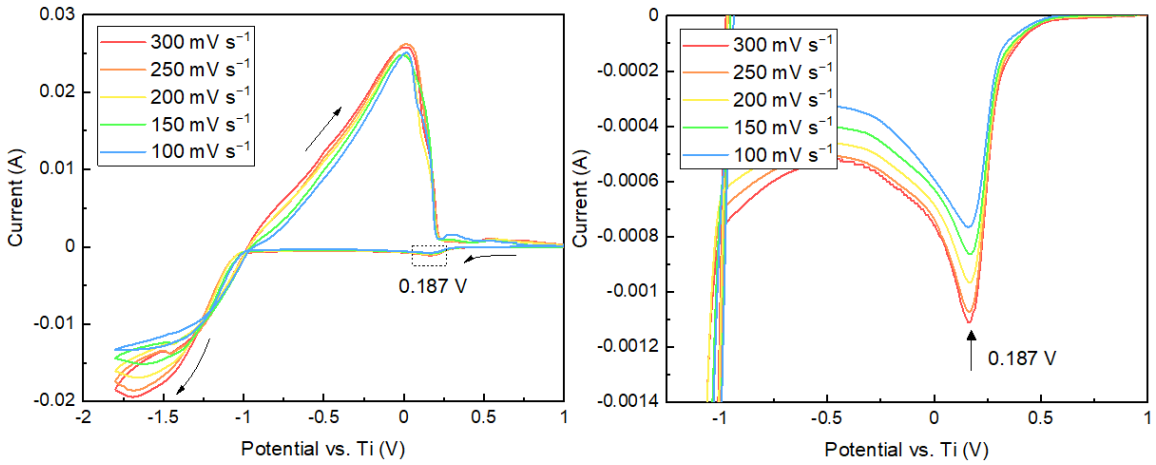

Figure 2. Cyclic voltammograms recorded at different scan rates from BMIC-$AlCl_3$ IL (0.667 $AlCl_3$ mole fraction) with 1.11987×10^{-2} mol L^{-1} $Ti[(Al_2Cl_7)_4]^{2-}$ ions at 383 K.

During the reverse sweep, a broad oxidation peak at −0.06V vs. Ti, followed by a tiny peak at 0.475 V vs. Ti, appears, which dictates the anodic stripping of Al and Ti complex species, respectively. The ratio of cathodic peak current (E_{pc}) and anodic peak current (E_{pc}) measured for reduction/oxidation reactions for Ti during the forward and reverse sweeps is close to unity (E_{pc}/E_{pa}~1). Moreover, the interpeak distance (ΔE_p) is 0.288 V. That is, $(\Delta E_p)=|E_{pc}-E_{pa}|=28.8$ mV. For an entirely reversible reaction, the $\Delta E_p=2.303RT/nF=59.2$ mV/n, where n represents the number of electrons exchanged during the reduction or oxidation reaction. The number of electrons involved in reduction or oxidation reaction according to the reaction [3] is 2. For the two-electron reduction or oxidation reaction, the value of ΔE_p should be 29.6 mV, which is close to the observed value of 28.8 mV. This suggests that the charge transfer processes involving deposition/stripping of Ti reversible.

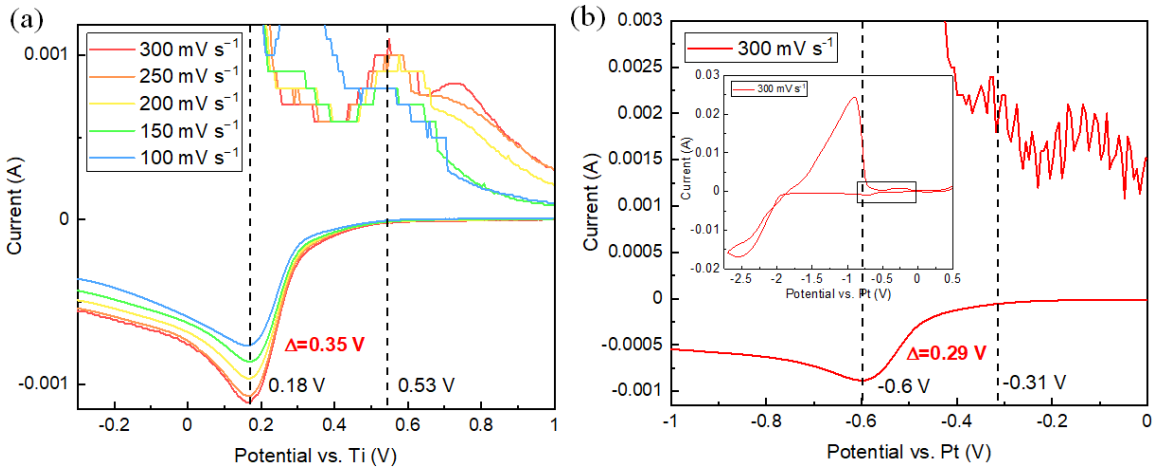

Figure 3. Cyclic voltammograms recorded from BMIC-$AlCl_3$ IL (0.667 $AlCl_3$ mole fraction) at 383 K versus (a) Ti at different scan rates (magnified view) and (b) Pt at the scan rate of 300 mV s^{-1} for comparison.

The reduction peak at −1.4 V vs. Ti and anodic stripping peak at −0.06 V vs. Ti in Figure 2 are separated by ΔE_p = ~1.34 V. Higher value of ΔE_p (> 59.2 mV/*n*, considering a three-electron reduction reaction, *n*=3) for Al deposition indicates that the electrochemical process is quasi-reversible. To further confirm the electrochemical deposition of Ti, cyclic voltammogram of BMIC-$AlCl_3$ ($AlCl_3$ mole fraction of 0.667) electrolyte was re-recorded on titanium wire using platinum reference electrode as shown in Figure 3(b). The reduction peak at −0.6 V vs. Pt (Figure 2b) confirms the deposition of Ti, which is in line with the reduction peak for Ti from [EMIm]Tf_2N containing 0.25 M $TiCl_4$ electrolyte (41). Alternatively, we performed the CV for BMIC-$AlCl_3$ IL with a 0.667-mole fraction of $AlCl_3$ without any Ti content. The CVs at different scan rates do not exhibit any reduction peaks in the regime of potentials where Ti redox peaks are observed from Ti-containing BMIC-$AlCl_3$ electrolyte.

As seen in Figure 2, the overall shapes of CVs for different scan rates are similar. However, there are noticeable shifts in the peak potentials for deposition of Al during cathodic sweeps. With an increase in scan rate, the reduction peak current increases. The reduction peak at 0.187 V vs. Ti signifying the reduction of $[Ti(Al_2Cl_7)_4]^{2-}$ to metallic Ti does not change with respect to the scan rate, as shown in the magnified view of the reduction peaks in Figure 3a. This suggests that this two-electron reduction reaction is a reversible process. No discernible shifts in anodic stripping peaks related to Al during anodic sweep are seen, although anodic stripping peaks for Ti shows irregular peak potentials due to complex electrochemistry involving quasi-reversible reaction. We rule out the possibility of the occurrence of redox peaks of Ti due to underpotential deposition (UPD). The deposition of metal on a substrate of the same material is deposited by the UPD process (42). The thickness of such materials deposited by UPD is of few monolayers. If it is due to the UPD process, then a considerable amount of Ti may not be deposited. The formation of the Ti-Al deposit (with ~3 at.% Ti at lower potential) from the same composition was confirmed from SEM-EDS previously (43). The cathodic reduction potentials are used for estimating the diffusion coefficients of $[Ti(Al_2Cl_7)_4]^{2-}$ anions. The diffusion coefficient for $Al_2Cl_7^-$ anions can also be estimated. However, our primary purpose in the present study is to investigate the electrochemical parameters for

the electrodeposition of Ti. Hence, we have focused on determining the diffusion coefficient calculation for $[Ti(Al_2Cl_7)_4]^{2-}$ anion species.

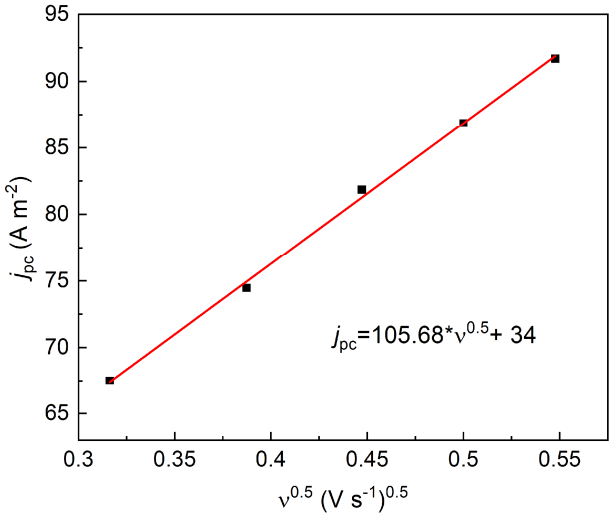

Figure 4. A plot of j_{pc} versus $\nu^{0.5}$ at 383 K (from redox peaks of Ti-species in BMIC-$AlCl_3$ IL).

To get insights into the rate of electron transfer or diffusion current (only the cathodic reaction considered), the diffusion coefficient of $[Ti(Al_2Cl_7)_4]^{2-}$ ions is calculated from the Randell–Sevcik relation (44),

$$j_{pc} = 0.4958nFC_i(\frac{\alpha nF}{RT})^{0.5}D^{0.5}v^{0.5} \quad [6]$$

where j_{pc} is the cathodic peak current density (obtained by dividing the current by area A of the working electrode), C_i is the bulk concentration of $[Ti(Al_2Cl_7)_4]^{2-}$ ions (*ca.* 1.11987 × 10^{-5} mol L^{-1}), R is the gas constant (8.314 J K^{-1} eq^{-1}), T is the experimental temperature (K), α is the charge transfer coefficient, n is the number of electrons transferred/molecule or ion (n=2), and F is the Faraday constant (96485 C mol^{-1}), D is the diffusion coefficient (m^2 s^{-1}), and ν is the scan rate (V s^{-1}). For quasi-reversible reaction, α can be determined by Nicholson and Shain relation (45) as,

$$\left|E_{pc} - E_{pc/2}\right| = 1.857RT/\alpha nF \quad [7]$$

where E_{pc} is the cathodic peak potential (V), and $E_{pc/2}$ is the cathodic half-peak potential (V). From Figure 4, the D can be calculated from the slope of a linear plot between cathodic peak current density (j_{pc}) versus $\nu^{0.5}$ once the C_i and α are known from the slope $0.4958nFC_i(\frac{\alpha nF}{RT})^{0.5}D^{0.5}$. The D value is calculated using the slope from Figure 4 and is listed in TABLE I, along with all the parameters obtained from CV curves.

TABLE I. Electrochemical parameters obtained from Figure 3(a) and Figure 4 at 383k. The area of a working electrode immersed in the liquid is 0.1178×10^{-2} m^2.

Scan rate ($mV\ s^{-1}$)	E_{pc} (mV)	$E_{pc/2}$ (mV)	E_{pa} (mV)	$\lvert E_{pc}-E_{pa}\rvert$ (mV)	$\lvert E_{pc}-E_{pc/2}\rvert$ (mV)	$\lvert j_{pc}\rvert$ ($A\ m^{-2}$)	α	D, $\times 10^{-10}$ ($m^2\ s^{-1}$)
100	86.85	205.23	246.15	159.30	118.38	65.2287	0.26	This work
150	97.90	209.61	342.60	244.69	111.71	72.1613	0.27	
200	103.45	211.70	433.30	329.84	108.24	78.5135	0.28	
250	109.00	220.05	430.50	321.50	111.05	82.2519	0.28	
300	114.56	223.64	452.44	337.88	109.08	85.4532	0.28	
						Average	0.27	9.74

Chronopotentiometry (CP)

Chronopotentiometry (CP) can be used to study the mechanism and kinetics of chemical reactions involving one or more redox species. CP method involves galvanostatic mode to control current and measure voltage. For systems involving only one redox species, an S-shaped current-voltage response is observed. The potential of the electrode changes from open-circuit potential to an approximately constant value, until the concentration of the redox species at the electrode is depleted. When this species is depleted at the electrode surface, the potential rapidly shifts to a potential that is able to sustain the applied current. This sudden shift is called the transition time (τ). If only one redox species is present, the potential shifts to a value that causes either the supporting electrolyte or solvent to be reduced/oxidized. If the redox process is reversible, the potential response during the plateau of the sigmoidal curve is controlled by the concentration of the oxidized and reduced forms of the redox couple at the electrode surface. Therefore, one can use the Nernst equation to evaluate the formal potential for the reduction process, as long as the diffusion coefficients of the oxidized and reduced form of the redox couple are known (46).

The quantitative relationship between transition time and current density using CP technique using the Sand equation (47) given by equation [8],

$$j\,\tau^{0.5} = 0.5nFCD^{0.5}\pi^{0.5} = constant \qquad [8]$$

The advantage of CP is that the Sand equation is appropriate for both planar and spherical electrodes to determine the diffusion coefficient, unlike the Cottrell equation (for CA method) representing the diffusion-controlled reaction. A better precision can be achieved using CP and Sand equation because the measured parameters τ and j vary linearly with D and non-linearly with $D^{0.5}$ for the Sand and Cottrell equations, respectively. The average value of the diffusion coefficient can be calculated by measuring the transition times at several current densities using equation [9] or from the slope of $\tau^{0.5}$ versus j,

$$D = \frac{4j^2\tau}{\pi\,(nFC)^2} \qquad [9]$$

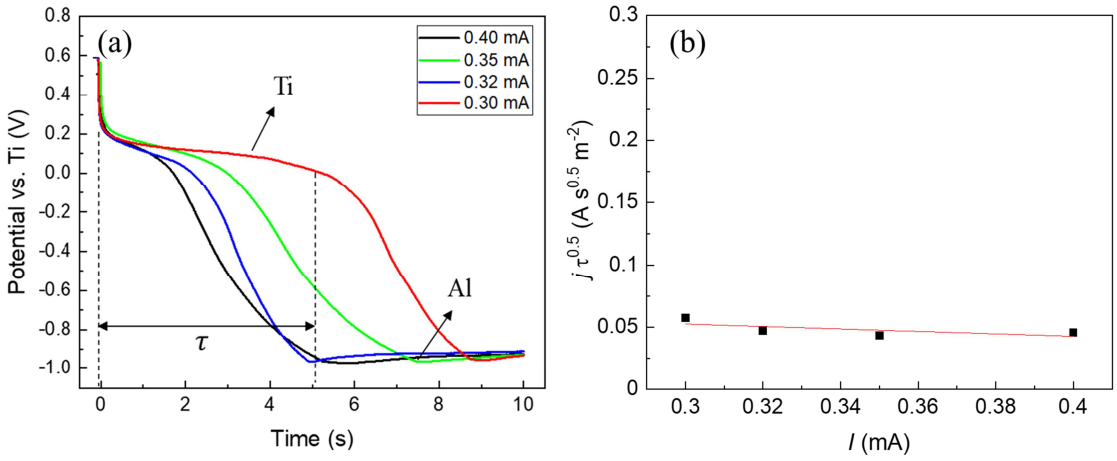

Figure 5. (a) Chronopotentiometric transients at different currents for 10 s duration at 383 K from BMIC-$AlCl_3$ IL and (b) Plot of $j\tau^{0.5}$ versus different applied currents.

Figure 5a shows the CP curves recorded for different currents, clearly revealing the distinct plateau regions for Ti and Al in the various potential regimes. Then, by plotting the transition time versus current density, as shown in Figure 5, the D values are estimated at 383 K. The average value of $j\tau^{0.5}$ at 383 K is 48.3 A $s^{0.5}$ m^{-2}, and the calculated D value is 6.36×10^{-10} m^2 s^{-1}. The D value calculated from the CV method is higher than that calculated by the CP method. The discrepancy could be because the CV method uses a modified Randles-Sevcik equation, which is a kinetically driven process. In contrast, the CP method uses the Scharifker-Hills and Cottrell equations, which is a static measurement.

Chronoamperometry (CA) and Nucleation and growth mechanism

The chronoamperometry (CA) study was performed to study the nucleation and growth mechanism of Ti or Ti-Al alloy deposits from BMIC-$AlCl_3$ (0.667 $AlCl_3$ mole fraction) containing 1.11987×10^{-2} mol L^{-1} of $[Ti(Al_2Cl_7)_4]^{2-}$ anions at 383 K. Since no nucleation peaks were observed near the reduction potential of Ti, the CA method was not used to estimate the D values. Figure 6 shows the CA plots at different overpotentials. The potentials were varied from −1.00 to −1.35 V *vs*. Ti, which was sufficient to initiate the nucleation and growth of Ti along with Al. The potentials higher than the deposition potentials of Ti were chosen because no nucleation peaks were noticed due to lower concertation of Ti species relative to that of Al-species in the ionic liquid. The current rises first due to the onset of nucleation and growth of the Ti and Al nuclei and then follows a current decay slowly after t_m (reaching a maximum peak) due to mass-transfer limitation (27).

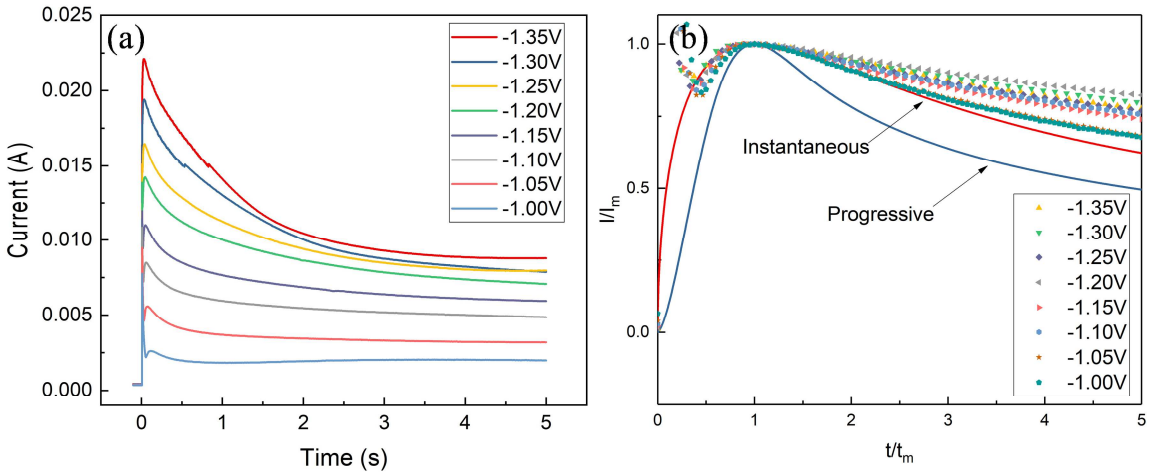

Figure 6. (a) Chronoamperometric current-time transients for TiAl deposition from BMIC-$AlCl_3$ IL with different overpotentials at 383 K. (b) Comparison of experimental current-time transients with simulated data using theoretical instantaneous and progressive nucleation model for BMIC-$AlCl_3$ IL with different overpotentials at 383 K.

In Figure 6a, as the potential increases, the value of I_m seems to increase while the value of t_m tends to decrease. This is due to the increase in nucleation rate and nucleation density (48). The maximum current and corresponding time values obtained from Figure 6a were further used to investigate the nucleation mechanism and diffusion coefficient of $[Al_2Cl_7]^-$ and $[Ti(Al_2Cl_7)_4]^{2-}$ anion species in the BMIC-$AlCl_3$ IL. It is known that the electrodeposition of metal follows a three-dimensional nucleation process at the initial stages. There are mainly two nucleation growth models, viz. instantaneous and progressive, as described by Scharifker and Hills (49). The dimensionless experimental current–time transients is compared with the dimensionless theoretically instantaneous and progressive nucleation model, which can be expressed by equations [10-11], which represent the relationship between dimensionless current density (j/j_m) to the dimensionless time (t/t_m).

$$\text{Instantaneous: } (j_{inst}/j_m)^2 = 1.9542(t_{inst}/t_m)^{-1}\{1 - exp[-1.2564(t_{inst}/t_m)]\}^2 \quad [10]$$

$$\text{Progressive: } (j_{prog}/j_m)^2 = 1.2254(t_{prog}/t_m)^{-1}\{1 - exp[-2.3367(t_{prog}/t_m)^2]\}^2 \quad [11]$$

where j is the current density (A m^{-2}) at any time t, j_m is the maximum current density at t_m time (s) where it occurs. To determine the nucleation mechanism of Ti-Al alloy in BMIC-$AlCl_3$ IL, the data from Figure 6a are compared with the theoretical instantaneous and progressive nucleation model. Such dimensionless current-time transients for different potentials at 383K along with theoretical nucleation processes are plotted and compared in Figure 6b. Hence, it is clear that the electrodeposition of Ti-Al alloy follows instantaneous nucleation at a lower temperature, suggesting a 3D instantaneous nucleation process.

Conclusions

The electrochemical behavior of titanium-chloroaluminate anion species in Lewis acidic BMIC-$AlCl_3$ ionic liquid with 0.667 $AlCl_3$ mole fraction is investigated by cyclic voltammetry (CV) and chronopotentiometry (CP) at 383K to calculate the diffusion coefficient (*D*). The *D* values obtained from CV and CP methods are 9.74×10^{-10} m^2 s^{-1} and 6.36×10^{-10} m^2 s^{-1}, respectively. Further, the nucleation and growth mechanism of Ti-Al alloy deposition from BMIC-$AlCl_3$ ionic liquid is studied from chronoamperometry (CA). The three-electron reduction process of $Al_2Cl_7^-$ to metallic Al is quasi-reversible, while the two-electron reduction of $[Ti(Al_2Cl_7)_4]^{2-}$ to metallic Ti is a reversible process. The CA study indicated that the nucleation of Ti-Al alloy is an instantaneous nucleation process.

Acknowledgments

The authors acknowledge the financial support from the National Science Foundation (NSF) award number 1762522 and ACIPCO for this research project. Authors also thank the Department of Metallurgical and Materials Engineering, the University of Alabama, for providing the experimental and analytical facilities.

References

1. W. Kroll, *Trans. Electrochem. Soc.*, **78**(1), 35 (1940).
2. K. H. Stern, in *Metallurgical and Ceramic Protective Coatings*, p. 9, Springer (1996).
3. D. Wei, M. Okido and T. Oki, *J. Appl. Electrochem.*, **24**(9), 923 (1994).
4. T. Oishi, H. Kawamura and Y. Ito, *J. Appl. Electrochem.*, **32**(7), 819 (2002).
5. J. H. Von Barner, P. Noye, A. Barhoun and F. Lantelme, *J. Electrochem. Soc.*, **152**(1), C20 (2004).
6. Y. Song, S. Jiao, L. Hu and Z. Guo, *Metall. Mater. Trans. B*, **47**(1), 804 (2016).
7. D. R. Sadoway, *JoM*, **43**(7), 15 (1991).
8. S. Hai-bin, Z. Xiu-rong, Z. Zhi-guo and H. Xue-hui, *J. Electrochem.*, **14**(1), 104 (2008).
9. C. Guang-Sen, M. Okido and T. Oki, *Electrochim. Acta*, **32**(11), 1637 (1987).
10. D. Pradhan and R. Reddy, Production of Al-Ti Alloys Using Ionic Liquid Electrolytes at Low Temperatures, in *Innovation in Titanium Technology: Novel Materials and Processes I*, p. 79, TMS, The Minerals, Metals and Materials Society (2007).
11. D. Pradhan and R. G. Reddy, *Electrochim. Acta*, **54**(6), 1874 (2009).
12. D. Pradhan, R. Reddy and A. Lahiri, *Metall. Mater. Trans. B*, **40**(1), 114 (2009).
13. M. Zhang, V. Kamavaram and R. G. Reddy, *Mining Metall. Explor.*, **23**(4), 177 (2006).
14. D. R. MacFarlane, M. Forsyth, E. I. Izgorodina, A. P. Abbott, G. Annat and K. Fraser, *Phys. Chem. Chem. Phys.*, **11**(25), 4962 (2009).
15. H. Weingaertner, *Angew. Chem. Int. Ed.*, **47**(4), 654 (2008).

16. J. D. Holbrey, W. M. Reichert, R. G. Reddy and R. D. Rogers, in *Ionic Liquids as Green Solvents: Progress and Prospects,* , R. D. Rogers and K. R. Seddon Editors, p. 121, ACS Symposium Series 856, American Chemical Society, New York (2003).
17. V. Kamavaram and R. G. Reddy, *Int. J. Therm. Sci.*, **47**(6), 773 (2008).
18. V. Kamavaram and R. G. Reddy, in *Light metals 2005*, H. Kvande Editor, p. 501, Warrendale (2005).
19. Ramana G. Reddy, Zhijing Zhang, Mario F. Arenas and Daniel M. Blake, *High. Temp. Mater. Proc.*, **22**(2), 87 (2003).
20. V. Karmavaram and R. G. Reddy, in *Aluminum 2003*, S. K. Das Editor, p. 299 (2003).
21. Y. Peng and R. G. Reddy, in *Advances in Molten Slags, Fluxes, and Salts: Proceedings of the 10th International Conference on Molten Slags, Fluxes and Salts 2016*, p. 1169 (2016).
22. T. Wang, S. Viswanathan, D. Mantha and R. G. Reddy, *Sol. Energy Mater. Sol. Cells*, **102**, 201 (2012).
23. R. Reddy, A. Yahya and L. Brewer, *J. Alloys Compd.*, **321**(2), 223 (2001).
24. M. Zhang, V. Kamavaram and R. G. Reddy, *J. Phase Equilib. Diff.*, **26**(2), 124 (2005).
25. M. M. Zhang and R. G. Reddy, *Min. Proc. Ext. Met.*, **119**(2), 71 (2010).
26. A. Liu, Z. Shi and R. G. Reddy, *Ionics*, **26**(6), 3161 (2020).
27. A. Liu, Z. Shi and R. G. Reddy, *Electrochim. Acta*, **251**, 176 (2017).
28. A. Liu, Z. Shi and R. G. Reddy, *J. Electrochem. Soc.*, **164**(9), D666 (2017).
29. M. Li, Z. Wang and R. G. Reddy, *J. Electrochem. Soc.*, **161**(4), D150 (2014).
30. P. Koronaios, D. King and R. A. Osteryoung, *Inorg. Chem.*, **37**(8), 2028 (1998).
31. V. Kamavaram, D. Mantha and R. G. Reddy, *Electrochim. Acta*, **50**(16), 3286 (2005).
32. Q. Liao, W. R. Pitner, G. Stewart, C. L. Hussey and G. R. Stafford, *J. Electrochem. Soc.*, **144**(3), 936 (1997).
33. Y. Zhao and T. VanderNoot, *Electrochim. Acta*, **42**(11), 1639 (1997).
34. T. Jiang, M. C. Brym, G. Dubé, A. Lasia and G. Brisard, *Surf. Coat. Technol.*, **201**(1-2), 1 (2006).
35. Z. J. Karpinski and R. A. Osteryoung, *Inorg. Chem.*, **23**(10), 1491 (1984).
36. D. Pradhan and R. G. Reddy, *Mater. Chem. Phys.*, **143**(2), 564 (2014).
37. J. Tang and K. Azumi, *Electrochim. Acta*, **56**(3), 1130 (2011).
38. T. Jiang, M. J. Chollier Brym, G. Dubé, A. Lasia and G. M. Brisard, *Surf. Coat. Technol.*, **201**(1), 1 (2006).
39. J. S. Wilkes, J. A. Levisky, R. A. Wilson and C. L. Hussey, *Inorg. Chem.*, **21**(3), 1263 (1982).
40. J. Tang and K. Azumi, *Electrochim. Acta*, **56**(3), 1130 (2011).
41. F. Endres, S. Zein El Abedin, A. Y. Saad, E. M. Moustafa, N. Borissenko, W. E. Price, G. G. Wallace, D. R. MacFarlane, P. J. Newman and A. Bund, *Phys. Chem. Chem. Phys.*, **10**(16), 2189 (2008).
42. A. Bakkar and V. Neubert, *Electrochem. Commun.*, **51**, 113 (2015).
43. P. S. Shinde, Y. Peng and R. G. Reddy, in, p. 1659, TMS 2020 149th Annual Meeting & Exhibition Supplemental Proceedings, Cham (2020).
44. A. J. Bard, L. R. Faulkner, J. Leddy and C. G. Zoski, *Electrochemical Methods: Fundamentals and Applications*, Wiley New York (1980).

45. R. S. Nicholson and I. Shain, *Anal. Chem.*, **36**(4), 706 (1964).
46. A. J. Bard and L. R. Faulkner, Fundamentals and Applications, New York: Wiley, 2001, in, Wiley & Sons (2001).
47. J. E. Baur, in *Handbook of Electrochemistry*, C. G. Zoski Editor, p. 829, Elsevier, Amsterdam (2007).
48. H. Yang and R. G. Reddy, *J. Electrochem. Soc.*, **161**(10), D586 (2014).
49. B. Scharifker and G. Hills, *Electrochim. Acta*, **28**(7), 879 (1983).